NINTH EUROPEAN ROTORCRAFT FORUM

Paper No. 8

THE DIFFERENCE BETWEEN THE EFFECTS OF PITCH AND PLUNGE ON DYNAMIC AIRFOIL STALL

L. E. ERICSSON AND J. P. REDING

Lockheed Missiles & Space Company, Inc.
Sunnyvale, California, USA

September 13-15, 1983

STRESA, ITALY

Associazione Industrie Aerospaziali

Associazione Italiana di Aeronautica ed Astronautica

THE DIFFERENCE BETWEEN THE EFFECTS OF PITCH AND PLUNGE ON DYNAMIC AIRFOIL STALL

L. E. Ericsson and J. P. Reding

Lockheed Missiles & Space Company, Inc.
Sunnyvale, California, USA

SUMMARY

It is well established that there is a strong coupling between airfoil motion and boundary layer separation. Less well known is the fact that this coupling differs greatly for a pitching and a plunging airfoil. An analysis shows this difference to be caused by different boundary conditions at the airfoil surface, the so called moving wall effects. Various experimental results are analyzed to illustrate how large this difference can become.

NOMENCLATURE

c	chord length
f	frequency
K_a	dynamic overshoot parameter, Eqs. (5) - (7).
l	section lift, coefficient $c_l = l/(\rho_\infty U_\infty{}^2/2)c$
m_p	section pitching moment, coefficient $c_m = m_p/(\rho_\infty U_\infty{}^2/2)c^2$
n	section normal force, coefficient, $c_n = n/(\rho_\infty U_\infty{}^2/2)c$
Re	Reynolds number based on chord length, $Re = U_\infty c/\nu_\infty$
t	time
U	horizontal velocity
x	chordwise distance from the leading edge
z	translatory coordinate, positive downward
α	angle of attack
$\bar{\alpha}$	equivalent angular amplitude, Eq.(1)
α_o	mean (trim) angle of attack
Δ	increment or amplitude
θ	perturbation in pitch
ξ	dimensionless x-coordinate, $\xi = x/c$
ρ	air density
ν	kinematic viscosity
ω	angular frequency, $\omega = 2\pi f$
$\bar{\omega}$	reduced frequency, $\bar{\omega} = \omega c/U_\infty$

Subscripts

CG	center of gravity or rotation axis
LE	leading edge
MAX	maximum
MIN	minimum
s	separation
vg	vortex growth
w	wake
W	wall
1.2	numbering subscript
∞	freestream conditions

1. INTRODUCTION

According to McCroskey's reviews of the subject of dynamic stall[1-4] the more and more extensive experiments have served to illustrate the great complexity of the dynamic stall phenomenon but have not led to the development of a satisfactory prediction method. One likely reason for this lack of progress is the assumption of equivalence between pitching and plunging motions. According to McCroskey's latest review[4] the present authors are alone in recognizing that there is a definite difference between the effects of pitching and plunging motions on the dynamic stall process[5]. New experimental results [6-8] demonstrate this vividly, as will be shown.

2. DISCUSSION

Based upon the experimental results published by Maresca et al [6] McCroskey[4] presented Fig. 1 to illustrate that for deep stall the equivalence principle appears reasonable, whereas it apparently does not work for light stall, according to Carta's results.[8]

Following Carta[8] we express the equivalent angle as follows:

$$\left.\begin{aligned} \alpha &= \alpha_o + \theta^* \\ \theta^* &= \bar{\alpha} \sin \omega t \\ \bar{\alpha} &= |\theta| = |\dot{z}|/U_\infty \end{aligned}\right\} \qquad (1)$$

where $\dot{z}/U_\infty$ is the "equivalent pitch".

Already in attached flow there will be a difference in the force generated at the same *instantaneous equivalent angle of attack* $\bar{\alpha}$. According to Ref. 9 the instantaneous lift will lag the instantaneous angle of attack with

$$\Delta\alpha_w = \xi_w c\dot{\alpha}/U_\infty \qquad (2)$$

where $\xi_w = 1.5$.

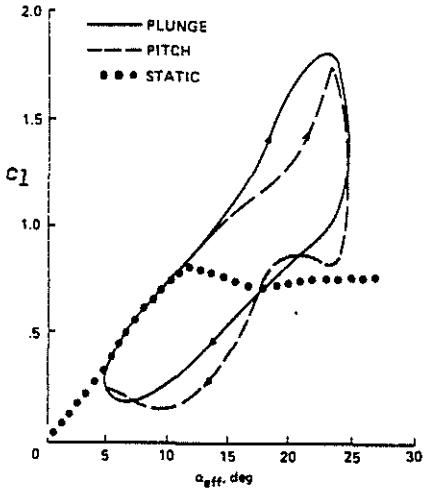

Fig. 1. Comparison of Pitch and Plunge Results in Deep Stall (Ref. 4)

This is the complete $\bar{\alpha}$-lag for the plunging airfoil. For the pitching airfoil there is a pitch rate-induced lift increment $\Delta c_l = c_{l\alpha}(1-\xi_{CG})\, c\dot{\alpha}/U_\infty$ giving an effective $\bar{\alpha}$-lag of

$$\Delta\alpha_{pitch} = \Delta\alpha_w - (1-\xi_{CG})\, c\dot{\alpha}/U_\infty \qquad (3)$$

For an airfoil pitching around the 25% chord, $\xi_{CG} = 0.25$, one obtains

$$\Delta\alpha_{pitch} = 0.5\Delta\alpha_{plunge} \qquad (4)$$

Thus, at $\alpha = \alpha_0$ the "up-and down-stroke" portions of the c_l or c_m loops should be twice as far apart for the plunging as for the pitching airfoil (for the same reduced frequency). Carta's test[8] gave this expected data trend. (Fig. 2)

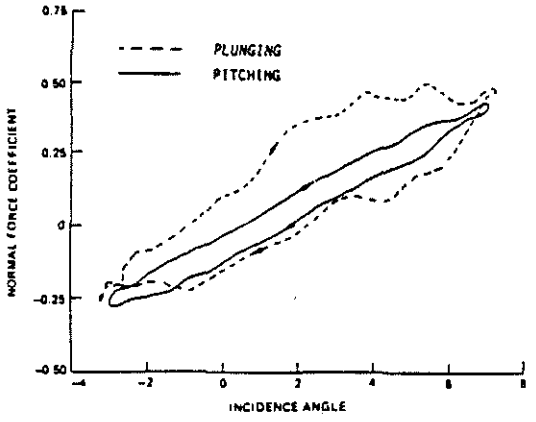

Fig. 2. Normal Force Pitch and Plunge Loops for $\alpha_0 = 2^0$, $\bar{\alpha} = 5^0$, and $\bar{\omega} = 0.5$ (Ref. 8)

2.1 Dynamic Stall Characteristics

The difference between the dynamic stall characteristics is a little more complicated. We have discussed in detail[5] how the dynamic overshoot of static $c_{l_{MAX}}$ is caused by two viscous flow effects (at moderate amplitudes and frequencies; there is an additional effect of the "spilled leading edge vortex" at large amplitudes and high frequencies[10]). One is the integrated effect of the time-lagged external pressure gradient on the boundary layer development, giving

$$\left.\begin{aligned}\Delta c_{ls1} &= c_{l\alpha}\,\Delta\alpha_{s1}\\ \Delta\alpha_{s1} &= K_{a1}\, c\dot{\alpha}/U_\infty\end{aligned}\right\} \qquad (5)$$

The other is the so called "leading edge jet" effect (Fig. 3). As the airfoil leading edge moves upward the boundary layer between stagnation and separation points experiences a moving wall/wall jet effect very similar to that observed on a rotating cylinder[11], as is sketched in the inset in Fig. 3. Thus, the boundary layer has a fuller profile than in the steady case and is therefore more difficult to separate. On the "downstroke" the effect is the opposite, promoting separation. It is shown in Refs. 5 and 9 how this effect is in a first approximation proportional to $\dot{z}_{LE}$. That is,

$$\left.\begin{aligned}\Delta c_{ls2} &= c_{l\alpha}\,\Delta\alpha_{s2}\\ \Delta\alpha_{s2} &= K_{a2}\,\dot{z}_{LE}/U_\infty\end{aligned}\right\} \qquad (6)$$

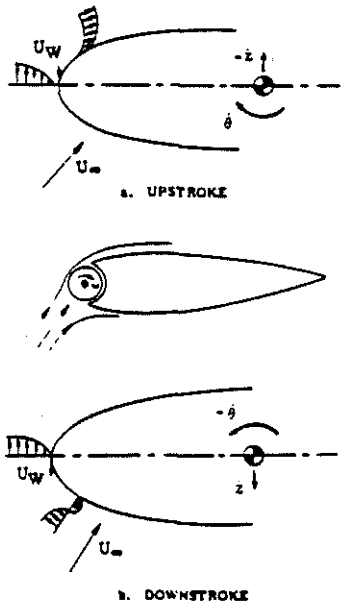

Fig. 3. "Leading Edge Jet" Effect

For the airfoil pitching around ξ_{CG} one obtains

$$\left.\begin{aligned} \Delta c_{ls} &= c_{l\alpha}\,\Delta\alpha_s \\ \Delta\alpha_s &= K_a\, c\dot{\alpha}/U_\infty \\ K_a &= K_{a1} + K_{a2}\,\xi_{CG} \end{aligned}\right\} \qquad (7)$$

These two mechanisms, Eqs. (5) and (6), which combine to give Eq. (7) for the pitching airfoil, are proportional to the dimensionless pitch and plunging rates, with the effects being opposite on the "downstroke" to what they are on the "upstroke". Recent experimental results[7] for pitch oscillations around the static stall angle illustrate this algebraic rate dependence (Fig. 4).

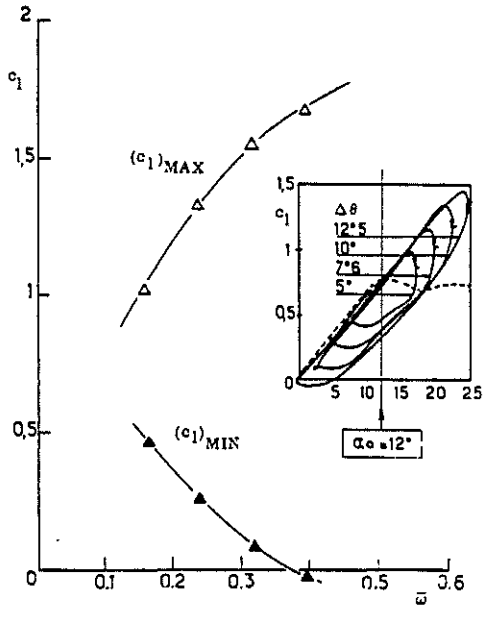

Fig. 4. Effect of Reduced Frequency on Maximum and Minimum Lift (Ref. 7)

Combining Eqs. (1) and (5) one finds that the pressure-gradient-lag effect is the same for pitching and plunging airfoils. However, the "leading edge jet" effects are of opposite kind, delaying separation for pitching and promoting it for plunging oscillations. This is well illustrated by the results obtained by Maresca et al[6], who designed plunging tests in accordance with Eq. (1) to provide the "equivalent pitch" results to be compared with the true pitch data obtained by Carr et al[12]. The moment characteristics (Fig. 5) reveal that the plunging airfoil stalls earlier than the pitching airfoil because of the adverse "leading edge jet" effect (Fig. 3). At stall a vortex is shed from the leading edge. This "spilled" vortex starts travelling downstream [10] at $\alpha_{VS} \approx 16^0$ for the plunging airfoil but is delayed until $\alpha_{VS} \approx 24^0$ for the pitching one (Fig. 5). According to the analysis in Ref. 10 the vortex-induced lift is proportional to $\sin^2 \alpha_{VS}$. With $\alpha_{VS} \approx 24^0$ and 16^0 respectively the vortex-induced lift should be twice as large for the pitching as for the plunging airfoil. It will be shown that the experimental results [6,12] exhibit this difference, contrary to what has been concluded by McCroskey [4] (Fig. 1)

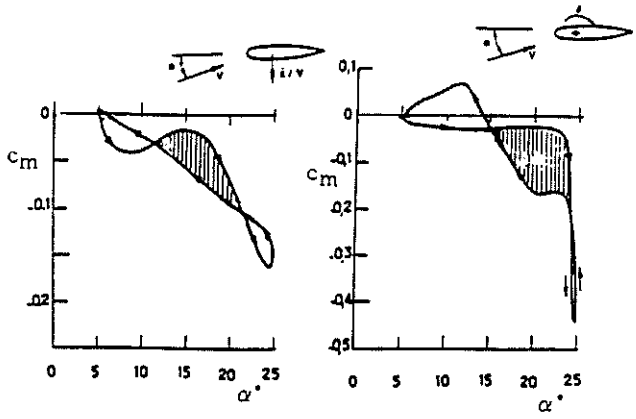

a. Plunging [6] b. Pitching [12]

Fig. 5. Pitching Moment Loops for Pitching and Plunging Oscillations (Ref. 6)

Figure 6 shows the experimental results [6,12] from which Fig. 1 was constructed. According to McCroskey[13] Maresca et al [6] based their decision to stretch the lift scale for the plunging airfoil on the large discrepancy between static characteristics for the two tests [6,12] (Fig. 7). The large difference in Reynolds

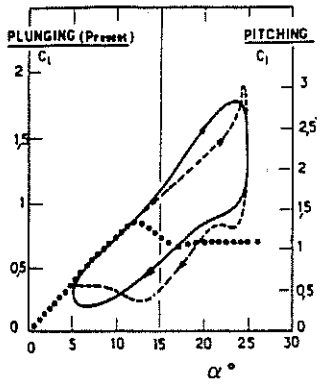

Fig. 6. Lift Loops for Pitching and Plunging Oscillations as presented in Ref. 6.

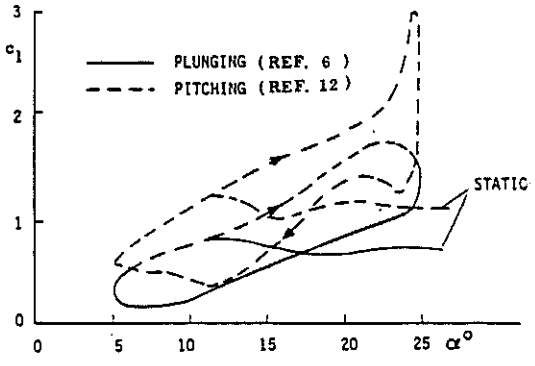

Fig. 7. Lift Loops of Fig. 6 plotted against a Common Lift Scale.

numbers, Re=0.25 x 10^6 for the plunging test [6] compared to Re=2.5 x 10^6 for the pitching airfoil[12], combined with differences between the two test facilities,was the likely cause, they thought, of the large difference in dynamic peak lift. However, it was shown in Ref. 14 that for large amplitudes and high frequencies the dynamic lift maximum for a pitching airfoil is independent of the static characteristics. This was demonstrated by using the experimental results obtained by Philippe[15] for a regular and a modified NACA-0012 airfoil (Fig. 8). The modified airfoil with its drooped leading edge has a much higher static $c_{l_{MAX}}$ than the regular airfoil, an effect similar to that of increasing the Reynolds number, as is discussed in detail in Ref. 14. The parameter $|\dot{\alpha}c/U_\infty| = \Delta\theta\,\bar{\omega}$ was even larger in the test performed by Maresca et al[6] than in that by Philippe[15]. Thus, the moving wall effects on the flow separation would have reached their saturation point for pitching oscillations in the facility used by Maresca et al[6]. Thus, one expects that if they had repeated the test of Carr et al[12], they would have measured the same dynamic lift maximum. Consequently, the difference between peak lift for plunging and pitching oscillations in Fig. 7 does not occur for the reasons believed by Maresca et al[6,13].

Another way to modify the results in Fig. 7 is to zero-shift them so they agree in the early attached-flow portion of the cycle (Fig. 9). One expects this agreement as there are no significant viscous flow effects there and the pitch-rate-induced camber effect discussed earlier is zero at the end of the cycle. As the pressure gradient time history is the same in the two tests, the differences in Fig. 9 are caused by different "leading edge jet" effects, as is illustrated by the insets. For the plunging airfoil the "leading edge jet" effect is zero at the mid portion, $\alpha = \alpha_0 = 15^0$, and reaches peak magnitude at the end points, $\bar{\alpha} = 15^0 + 10^0$. The effect is adverse at high angles of attack, $15^0 < \bar{\alpha} < 25^0$, and favorable at low angles, $5^0 < \bar{\alpha} < 15^0$. In contrast, the pitching airfoil experiences the peak "L.E. jet" effect at midpoint, favorable on the "upstroke" and adverse on the "downstroke", with the effect becoming zero at the end points. This explains the difference between the two loops in Fig. 9. On the "upstroke" favorable, large "L.E. jet" effects delay separation on the pitching airfoil compared to the plunging airfoil, for which the "L.E. jet" effects become adverse for $\alpha > \alpha_0$. As a consequence the "spilled leading edge vortex" is much stronger for the pitching than for the plunging airfoil, explaining the large difference in dynamic $c_{l_{max}}$ in the two cases. As was discussed earlier, one expects the vortex-induced lift to be twice as large for the pitching as for the plunging airfoil.

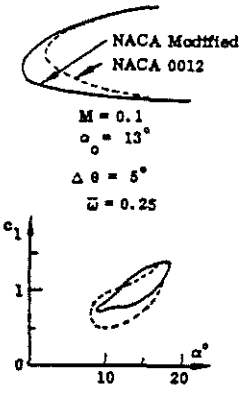

Fig. 8. Effect of Drooped Leading Edge on Dynamic Lift Loop (Ref. 15).

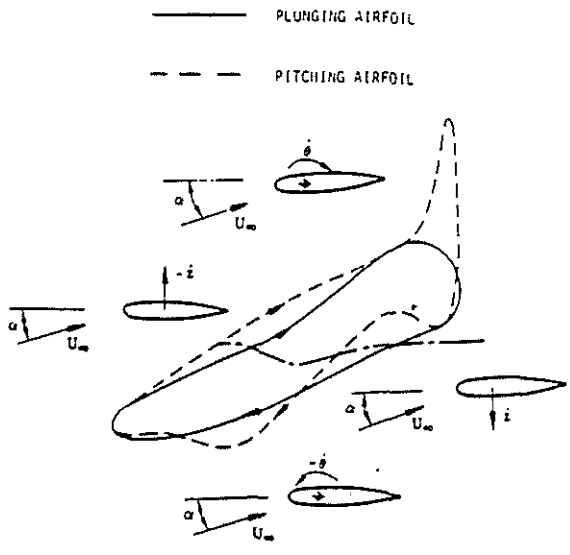

Fig. 9. "Leading Edge Jet" Effects on Pitching and Plunging Airfoils.

2.2 Damping in Plunge

In the inviscid (attached flow) region the damping derivative for plunging oscillations is simply

$$c_{n\dot{z}} = c_{n\alpha} \qquad (8)$$

In the stall region the only viscous contribution comes from the "leading edge jet" effect, Eq. (6). In view of these simple relationships one may wonder how the experimental results [8,16,17] in Fig. 10 can be explained. The corresponding static force characteristics shown in Fig. 11 give part of the answer. It is shown in Ref. 1 how the undamping in plunge measured by Liiva[17] (Fig. 10 b) can be generated by the adverse "leading edge jet" effects on the plunging "down stroke", provided that the static stall characteristics have a discontinuity and/or an angle of attack hysteresis. Comparing Figs. 10 and 11 one finds that a

damping degradation is only obtained in Liiva's test (Fig. 10b), in which case the static characteristics indicate the presence of a c_n-discontinuity (Fig. 11b).

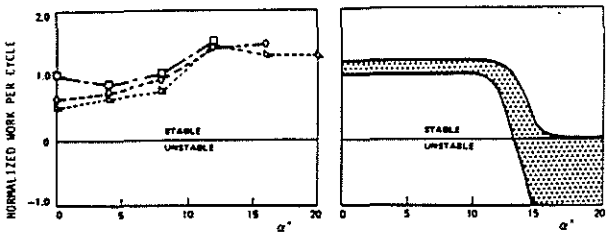

a. Rainey (Ref.16) b. Liiva et al (Ref.17)

Fig. 10. Normalized work per Cycle for Plunging Oscillations (Ref. 8)

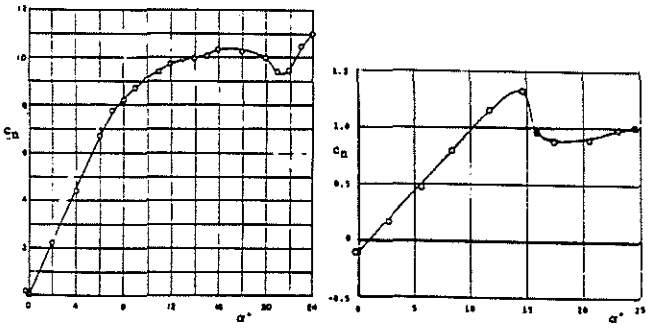

a. Rainey (Ref.16) b. Liiva et al (Ref.17)

Fig. 11. Static Force Characteristics (Ref. 8)

The comparison in Fig. 10 was made by Carta[8], whose test results showed the same data trend as Rainey's[16] (Fig. 10a); i.e. the damping at stall penetration exceeded the attached flow damping. Carta's static airfoil characteristics give a hint of the reason for this anomalous behavior[8] (Fig. 12), showing that the stall-induced lift loss is disappearing with increasing Reynolds number. It was shown in Ref. 11 that the upstream moving wall effect could promote boundary layer transition and cause a reversal of the Magnus lift generated by a rotating cylinder[18] (Fig. 13). Thus, the adverse "leading-edge-jet" effect on the plunging downstroke could cause earlier transition, thereby changing the flow separation from laminar to turbulent stall.

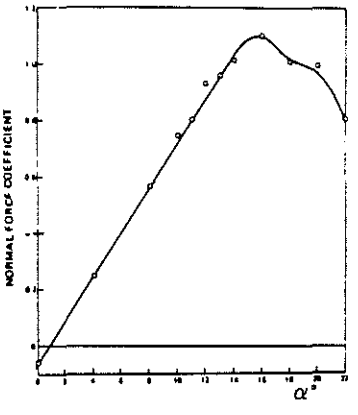

a. Re = 0.315 x 10^6

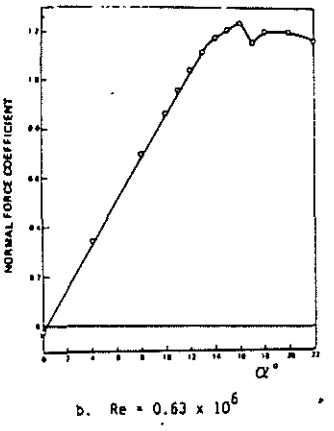

b. Re = 0.63 x 10^6

Fig. 12. Normal Force Characteristics of the SC 1095 Airfoil (Ref. 8)

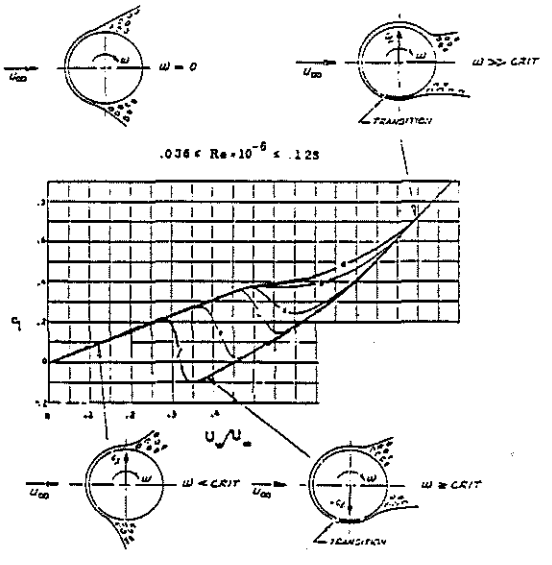

Fig. 13. Moving Wall Effects on a Circular Cylinder in Laminar Flow (Ref. 11)

Strong coupling between the airfoil motion and boundary Layer transition has been demonstrated for pitch oscillations[19] (Fig. 14). The moving wall effects, favorable on the upstroke and adverse on the downstroke, cause transition to occur at $\xi \approx 0.10$ at $\alpha \approx 5^0$ for decreasing α compared to at $\alpha \approx 9^0$ for increasing α. For plunging oscillations the effects are reversed, and the earlier transition would occur for increasing rather than for decreasing $\bar{\alpha}$. Carta's hot film response data[8] tend to verify this (Fig. 15). Comparing the results for pitch and plunge it can be seen how the adverse moving wall effect $\dot{z}(t)$ promotes transition and causes the plunging airfoil to have a longer run of attached turbulent flow prior to stall. As a result the flow stays attached past 7.5% chord whereas flow separation occurs forward of 5% chord on the pitching airfoil.

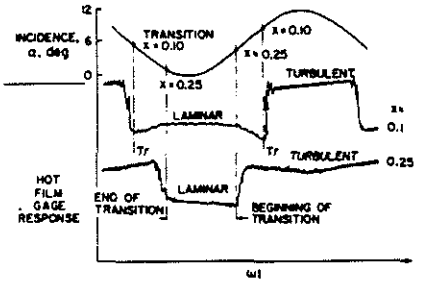

Fig. 14. Boundary Layer Transition on a Pitching Airfoil (Ref. 19)

The effect on the plunging $c_l(\alpha)$ loop of the coupling between airfoil motion and boundary layer transition just discussed can be visualized using the static data[20] in Fig. 16. Instead of causing the discontiguity to be caught, e.g. for Re = 0.66 x 10^6, the adverse "leading edge jet" effect on the plunging "downstroke" elevates the lift from for example Re = 0.33 x 10^6 to Re = 0.66 x 10^6, causing the area enclosed by the plunging loop to be larger than for attached flow, where this unsteady viscous flow effect is absent. The effect on the pitching moment of the opposite moving wall effects on transition for true pitch and equivalent pitch are even greater[8] (Fig. 17). The figure shows how the favorable "leading edge jet" effect on the plunging "backstroke" causes early flow reattachment, whereas the adverse effect during the pitching "backstroke" delays flow reattachment to an angle of attack below the static stall angle. These are the expected moving wall effects on flow reattachment. The corresponding effects on flow separation would cause earlier stall for the plunging than for the pitching airfoil during the "upstroke". The delayed stall for the plunging airfoil is caused by the moving wall effects on transition discussed earlier.

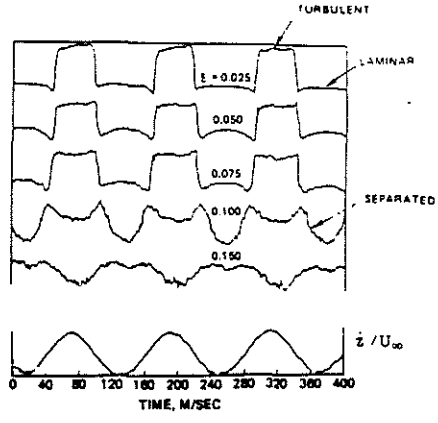

a. Plunging

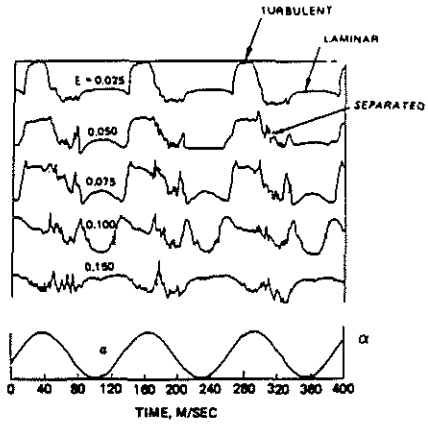

b. Pitching

Fig. 15. Hot Film Response for Pitching and Plunging Oscillations at $\alpha_o = 15^0$, $\bar{\alpha} = 5^0$, and $\bar{\omega} = 0.5$ (Ref. 8)

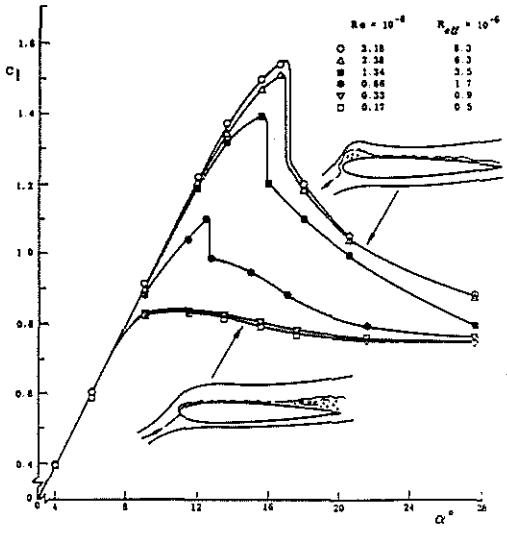

Fig. 16. Effect of Reynolds Number on the Lift Characteristics of the NACA-0012 Airfoil (Ref. 20).

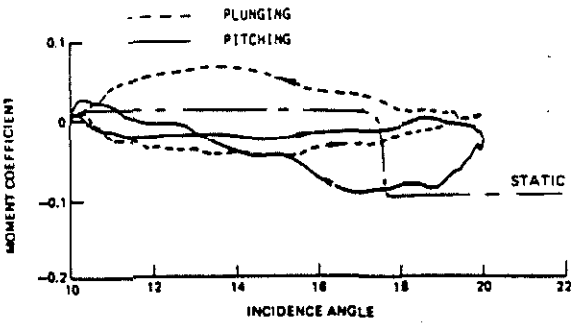

Fig. 17. Pitching Moment Loops for Pitching and Plunging Oscillations, $\alpha_o = 15^o$, $\bar{\alpha} = 5^o$, and $\bar{\omega} = 0.5$ (Ref. 8)

2.3 Utilization of Subscale Test Data

For the foreseeable future the prediction of dynamic stall characteristics will depend heavily upon the use of experimental results, usually obtained on subscale models. Great care has to be exercized when using the data for prediction of full scale dynamic characteristics. They can be used most effectively to verify mathematic models for the inter-relationship between dynamic and static characteristics, the unsteady flow concepts discussed in the present paper. Using these modules "analytic extrapolation" to full scale vehicle dynamics can be accomplished[21].

Carta's results[8] provide a good illustration of the care necessary when utilizing subscale test data. A casual user could draw the conclusion that the tested Sikorsky SC1095 airfoil was immune to the dynamic plunging instability experienced by the Vertol 23010-1,58 and NACA-0012 airfoils tested by Liiva[17]. This would, of course, be a serious misinterpretation of the experimental results, which in spite of troublesome wall interference effects[22], at least for low frequency data[23,24], provide the detailed information needed to clarify and verify the adverse moving wall effect on boundary layer transition for a plunging airfoil, a very important building block in our assembly of unsteady flow methodology.

The relationship between dynamic and static stall characteristics is complicated by the fact that different static load components have different phase lags[1]. This can be especially mystifying in the case of the pitching moment loops and associated damping. Without actually examining the different unsteady flow components the experimental results may appear to indicate that "the pitch damping behavior is not necessarily related to the static-stall behavior"[25]. For example, Carta's data[8] shown in Fig. 17 could be misinterpreted in this way. The static stall data are the same, and according to the general consensus, with one exception[5], there should be no difference between true and equivalent pitch results[4]. However, the experimental results show conclusively that there is a great difference between the dynamic effects of pitching and plunging. In general, the difference is caused by the opposite moving wall effects on flow separation. In this particular case the picture was complicated by the "leading edge jet" effects on boundary layer transition.

Detailed experimental investigations such as those performed by Maresca et al[6,7,26,27] Carta[8,28], and McCroskey et al[12,29,30] can provide the detailed checks needed of the unsteady flow concepts before they can be combined with static experimental results as described in Ref. 15 to permit "analytic extrapolation" to full scale dynamic stall characteristics. This appears at the present to be the only feasible means of determining what the full scale flight dynamics will be, short of flight testing. To the tunnel-peculiar effects already discussed, which make subscale dynamic simulation difficult[14,22], one has to add that based upon the present study the earlier assumed equivalence between the results for a pitching airfoil in a steady stream and those for a fixed airfoil in an oscillating stream does not hold when viscous flow effects are important, as in the case of dynamic stall.

3. CONCLUSIONS

A critical examination of earlier developed unsteady flow concepts for dynamic stall analysis in light of recent experimental results reveals the following:

- The new experimental results prove conclusively the existence of the so called "leading edge jet" effect, which can explain the observed differences between plunging and pitching airfoil characteristics.
- The main conclusion to be drawn from this study is that the analytic building blocks are now largely at hand for the assembly of a reliable method for prediction of dynamic stall characteristics through analytic extrapolation from subscale test data.

4. REFERENCES

1. McCroskey, W. J., "Recent Developments in Dynamic Stall", Proc. Univ. Ariz./USAF OSR Symposium on Unsteady Aerodynamics, Kinney, R. B. ed., Tuscon, March 1975, pp. 1-33.

2. McCroskey, W. J., "Some Current Research in Unsteady Aerodynamics - A Report from the Fluid Dynamics Panel", Paper 24, 46th Meeting of AGARD Propulsion and Energetics Panel, Monterey, Calif., Sept. 1975.

3. McCroskey, W. J., "Prediction of Unsteady Separated Flows on Oscillating Airfoils", AGARD LS-94, February 1978.

4. McCroskey, W. J., "The Phenomenon of Dynamic Stall", NASA TM 81264 and Paper 2, VKI Lecture Series 1981-4, March 1981.

5. Ericsson, L. E. and Reding, J. P., "Dynamic Stall Analysis in Light of Recent Numerical and Experimental Results", J. Aircraft, Vol. 13, No. 4, April 1976, pp. 248-255.

6. Maresca, C. A., Favier, D. J., Rebont, J. M., "Unsteady Aerodynamics of an Airfoil at High Angle of Incidence Performing Various Linear Oscillations in a Uniform Stream", J. Am. Helicopter Soc., April 1981, pp. 40-45.

7. Favier, D., Rebont, J., Maresca, C., "Profil d'Aile a Grande Incidence Animé d'un Mouvement de Pilonnement", 16eme Colloque d'Aerodynamique Appliquee, Lille, 13-15 November 1979.

8. Carta, F. O., "A Comparison of the Pitching and Plunging Response of an Oscillating Airfoil", NASA CR 3172, October 1979.

9. Ericsson, L. E. and Reding, J. P., "Unsteady Airfoil Stall, Review and Extension", J. Aircraft, Vol. 8, August 1971, pp. 609-616.

10. Ericsson, L. E. and Reding, J. P., "Dynamic Stall at High Frequency and Large Amplitude", J. Aircraft, Vol. 17, No. 3, March 1980, pp. 136-142.

11. Ericsson, L. E., "Karman Vortex Shedding and the Effect of Body Motion", AIAA Journal, Vol. 18, No. 8, August 1980, pp. 935-944.

12. Carr, L. W., McAlister, K. W., and McCroskey, W. J., "Analysis of Development of Dynamic Stall Based on Oscillating Airfoil Experiments", NASA TN D8382, 1977.

13. McCroskey, W. J. Private Communication, July 18, 1983.

14. Ericsson, L. E. and Reding, J. P., "Scaling Problems in Dynamic Tests of Aircraft-Like Configurations", Paper 25, AGARD-CP-227, February 1978.

15. Philippe, J. J. "LeDecrochage Instationnaire d'un Profil", ONERA TP No. 936, 1968.

16. Rainey, A. G., "Measurement of Aerodynamic Forces for Various Mean Angles of Attack on an Airfoil Oscillating in Bending with Emphasis on Damping in Stall", NACA Report 1305 (1957).

17. Liiva, J., "Unstedy Aerodynamic and Stall Effects on Helicopter Rotor Blade Airfoil Sections", J. Aircraft, Vol. 6, No. 1, Jan-Feb. 1969, pp. 46-51.

18. Swanson, W. M. "The Magnus Effect: A Summary of Investigations to date", J. Basic Eng., Vol. 83, Sept. 1961, pp 461-470.

19. McCroskey, W. J. and Philippe, J. J., "Unsteady Viscous Flow on Oscillating Airfoils", AIAA Journal, Vol. 13, No. 1, Jan. 1975, pp. 71-79.

20. Jacobs, E. N. and Sherman, A., "Airfoil Section Characteristics as Affected by Variations in the Reynolds Number", NACA Tech. Report 586 (1937).

21. Ericsson, L. E. and Reding, J. P., "Analytic Extrapolation to Full Scale Aircraft Dynamics", AIAA Paper 82-1387, Aug. 1982.

22. Ericsson, L. E. and Reding, J. P., "Dynamic Stall Simulation Problems", J. Aircraft, Vol. 8, No. 7, July 1971, pp. 579-583.

23. Ericsson, L. E. and Reding, J. P., "Quasi-Steady and Transient Dynamic Stall Characteristics" Paper 24, AGARD CP-204, Sept. 1976.

24. McCroskey, W. J., Carr, L. W., and McAlister, K. W., "Dynamic Stall Experiments on Oscillating Airfoils", AIAA Journal, Vol. 14, No. 1, Jan. 1976, pp. 57-63.

25. McCroskey, W. J., McAlister, K. W., Carr, L. W., Pucci, S. L., Lambert, O., and Indergrand, R. F., "Dynamic Stall on Advanced Airfoil Sections", J. Am. Helicopter Soc., July 1981, pp. 40-50.

26. Maresca, C. A., Favier, D. J., Rebont, "Experiments on an Airfoil at High Angle of Incidence in Longitudinal Oscillations", J. Fluid Mech., (1979), Vol. 92, Part 4, pp. 671-690.

27. Maresca, C., Rebont, J., and Valensi, J., "Separation and Reattachment of the Boundary Layer on a Symmetric Airfoil Oscillating at a Fixed Incidence in Steady Flow", Proc. Univ. Ariz/USAF OSR Symposium on Unsteady Aerodynamics, Kinney, R. B. ed., Tuscon, 1975, pp. 35-54.

28. Carta, F. O., "Analysis of Oscillatory Pressure Data Including Dynamic Stall Effects", NASA CR-2394, May 1974.

29. McAlister, K. W., Carr, L. W. and McCroskey, W. J., "Dynamic Stall Experiments on the NACA 0012 Airfoil, NASA TP 1100, Jan. 1978.

30. McCroskey, W. J., McAlister, K. W. Carr, L. W., and Pucci, S. L., "An Experimental Study of Dynamic Stall on Advanced Airfoil Sections Volume 1, Summary of the Experiment", NASA TM 84245, July 1982.